



Published in final edited form as:

Nat Immunol. 2016 March ; 17(3): 315–322. doi:10.1038/ni.3330.

A Septin Requirement Differentiates Autonomous- and Contact-Facilitated T Cell Proliferation

Adriana M. Mujal¹, Julia K. Gilden^{1,3}, Audrey Gérard¹, Makoto Kinoshita², and Matthew F. Krummel¹

¹Department of Pathology, University of California, San Francisco, 513 Parnassus Ave, HSW512, San Francisco, CA 94143-0511, USA

²Division of Biological Sciences, Nagoya University Graduate School of Science, Furo, Chikusa, Nagoya 464-8602, Japan

Abstract

T cell proliferation is initiated by T cell antigen receptor (TCR) triggering and/or by soluble growth factors. In characterizing T cells lacking the septin cytoskeleton, we found that successful cell division has discrete septin-dependent and -independent pathways. Septin-deficient T cells failed cytokinesis when prompted by pharmacological activation or cytokines. In contrast, cell division was independent of septins when cell-cell contacts, such as those from antigen-presenting cells, provided a niche. This septin-independent pathway was mediated by phosphatidylinositol-3-OH kinase activation through a combination of integrins and co-stimulatory signals. We could differentiate cytokine- versus antigen-driven expansion *in vivo* and thus demonstrate that targeting septins has strong potential to moderate detrimental bystander or homeostatic cytokine-driven proliferation without influencing expansion driven by conventional antigen-presentation.

Introduction

T cell proliferation rapidly expands the number of antigen-specific cells, which is necessary to control infection. Typically, this kind of cell division is initiated by a T cell interaction with its cognate antigen on an antigen-presenting cell (APC), and its magnitude is determined by the strength of the T cell antigen receptor (TCR) recognition event in that cell-cell contact^{1–3}. Antigen-specific T cell clonal expansion has been reported to occur in the lymph node where swarming T cells engage in cell-cell contacts with proximal APCs and other activated T cells^{4,5}, and this may represent a ‘niche’ for cell division. Yet, cell

Users may view, print, copy, and download text and data-mine the content in such documents, for the purposes of academic research, subject always to the full Conditions of use:http://www.nature.com/authors/editorial_policies/license.html#terms

Correspondence should be addressed to: M.F.K. (Email: matthew.krummel@ucsf.edu)

³Current address: Department of Medical Microbiology and Immunology, University of Wisconsin School of Medicine and Public Health, Madison, WI 53706, USA.

AUTHOR CONTRIBUTIONS

A.M.M. and M.F.K. designed the experiments for all primary text figures; A.M.M. did these experiments; J.K.G. performed or participated in experiments related to initial characterization of *Sept7* KO mice; A.G. contributed to experimental design/analysis; M.K. provided the *Sept7*^{fllox/fllox} mice and consulted on experiments; and A.M.M. and M.F.K. wrote and revised the manuscript.

COMPETING FINANCIAL INTERESTS

The authors declare no competing financial interests.

division can also be driven by high local cytokine concentrations in the environment, in the possible absence of such cell-cell interaction. This scenario is considered a possible hazard for autoimmunity, as when non-virus-specific ‘bystander’ cells experience high concentrations of cytokines produced by viral-specific T cells during an immune response in a lymph node^{2,6}. Cytokine-driven cell division is also clearly important for homeostatic maintenance whereby cytokines such as interleukin 7 (IL-7) or IL-15, in conjunction with transient low-affinity peptide-MHC (p-MHC)–TCR interactions, support turnover of clones⁷. While asymmetric cell division has been proposed to be a pathway that can influence the individuality of daughter cells⁸, completion of cytokinesis has been considered invariant. To our knowledge, it has not previously been possible to clearly separate cytokine-versus TCR-driven cell division.

The physical event of cell division requires multiple processes, including the functions of specific kinases⁹, specific cytoskeletal proteins such as myosins and, notably, septins^{10–13}. Septins are a family of GTP-binding proteins that self-assemble into tetrameric, hexameric, or octameric quaternary structures and further into large filaments, rings, and gauzes *in vitro* and *in vivo*, and are assembled on the cell cortex^{14–16}. The mammalian septins, 13 in number, can be divided into four groups with one from each class required to form a canonical complex. In mammals, Septin 7, the only one in its class, appears indispensable for the generation of filaments, and its depletion leads to loss of the other septin proteins^{14,17–19}, presumably as a result of quality control processes.

Septins were originally identified as ‘cell division cycle’ (cdc) mutations²⁰ and are evolutionarily conserved in their critical role for cytokinesis. Similar to yeast, septins in mammals have been found to be essential for completion of cytokinesis^{12,21}. Septins are usually, but not exclusively, found assembled as a ring at the cleavage furrow^{12,22}. They previously have been suggested to be essential at the furrow to coordinate myosin motor proteins during cell abscission^{10,23}, to remodel the membrane as cytokinesis progresses²⁴, and to anchor the midbody ring structure to the membrane²⁵ as mother and daughter cell separation is resolved.

One exception to the requirement of septins for mammalian cytokinesis has been T cells; we showed that Septin 7 depletion in cell lines led to loss of the other septins, but resulted in near-normal cell division in response to cues driven by APCs¹⁷. T cell cytokinesis in the absence of septins was also recently confirmed in a *Sept7* genetic knockout model¹⁹. To investigate how T cells might evade this highly conserved requirement, we generated T cell-specific depletion of Septin 7 in mice and examined CD8⁺ T cell activation and functions under a variety of conditions. We unexpectedly found that septins are required differentially for T cell division, depending on whether or not T cells engaged in cell contacts during the period of cytokinesis. This finding led us to examine how proliferation occurs in septin-null CD8⁺ T cells so as to isolate the compensatory pathways. Our results provide a rare insight into the possibility of specifically attenuating cytokine-driven expansion while leaving antigen-driven expansion untouched.

Results

Development of Septin-deficient T cells is Intact

T cells were engineered to lack all septins using a *Cd4*-Cre allele in a genetic background of *Sept7^{flox/flox}* (*Sept7cKO*)¹⁹. These mice were subsequently crossed to the OT-I TCR-transgenic allele. Mice from both polyclonal or OT-I backgrounds demonstrated near-complete loss of Septin 7 in peripheral T cells with a small proportion (5–10%) of ‘escapees’ as assessed by flow cytometry (Supplementary Fig. 1a). To remove this contaminating population, we took care in all future analyses to eliminate these “escapees” from our experimental analysis when possible: either by detection of intracellular Septin 7 or use of mTmG mice²⁶ wherein Cre recombinase activity converts mTomato⁺ cells to mGFP⁺. As predicted from shRNA studies in cell lines¹⁷, genetic deletion of Septin 7 led to coordinate loss of other key T cell-expressed septin family members in peripheral T cells as assessed by immunoblotting (Supplementary Fig. 1b). The *Cd4*-Cre allele is expressed in a pre-DP phase of thymic development²⁷ and we observed initial onset of septin loss in DN thymocytes with maximal loss by the single-positive stage in *Sept7cKO* mice (Supplementary Fig. 1c). We observed comparable proportions of DN, DP, and SP thymocyte populations (Supplementary Fig. 1d), equivalent cellularity in secondary lymph node organs (Supplementary Fig. 1e), and similar frequency of CD4⁺ and CD8⁺ T cells within those organs (Supplementary Fig. 1f). Additionally, naïve resting septin-deficient CD8⁺ T cells maintained normal amounts of filamentous actin (Supplementary Fig. 1g) and septin-deficient OT-I T cells exhibited morphological defects that phenocopied previous findings with septin knockdown in T cell clones^{17,22} (Supplementary Fig. 1h,i). Together this demonstrates that development of septin-deficient T cells in this mouse model is largely intact.

Selective Proliferation Defects in Absence of Septins

We sought to examine T cell proliferation in the context of control or *Sept7cKO* CD8⁺ T cells isolated from these mice. Although septins are required for cell division in various types of eukaryotic cells, we and others have found that T cells proficiently proliferate in the absence of Septin 7 and associated septin family members^{17,22,19}. Consistent with this, we found that, when co-cultured *in vitro* with bone marrow-derived dendritic cells (BMDCs) pulsed with the OT-I peptide antigen SL8, CD8⁺ OT-I T cells diluted CFSE (Fig. 1a, Supplementary Fig. 2a), progressed in cell cycle, and expanded in numbers at a similar rate to wild-type cells (Fig. 1b). Unexpectedly, however, when activated with plate-coated anti-TCR antibody or soluble phorbol myristate acetate (PMA) and ionomycin, septin-deficient OT-I T cells underwent fewer cell divisions as assessed by CFSE dilution (Fig. 1a, Supplementary Fig. 2a) and by cell recovery (Fig. 1b) after 72 h. Polyclonal CD8⁺ *Sept7cKO* T cells exhibited these cell division defects as well (data not shown). Additionally, whereas stimulation with BMDCs generated largely conventional G1-S-G2/M cell cycle profiles, stimulation in the absence of APCs resulted in bi- and multi-nucleated cells, as detected by flow cytometry (Fig. 1a, Supplementary Fig. 2b) and confocal microscopy (Fig. 1c). This differential block in cell division was also observed in accumulation of septin-deficient forward-scatter^{hi} cells as compared to the septin-competent “escapees” from *Sept7cKO* OT-I mice in T cell cultures stimulated with anti-TCR or PMA

and ionomycin (Supplementary Fig. 2c). Altogether, this data demonstrates that T cells are not intrinsically unique in not requiring septins for cytokinesis, as was recently proposed¹⁹, but rather that only certain cytokinetic pathways are septin-independent. Moreover, in assessing how the generation of multinucleate cells relates to cell division, we observed that septin-deficient cells are susceptible to cytokinesis failure with every division, not simply the first (Fig. 1d). This observation argues that failure to divide is a stochastic event with the limited expansion of *Sept7*KO T cells to APC-independent stimuli resulting from a breakthrough event with each division.

The division defect was not an obvious result of differential loss of filamentous actin with some stimuli and not others, as phalloidin staining at 24 h was identical between *Sept7*KO and control OT-I cells (Supplementary Fig. 2d). Additionally, proximal signaling in response to all cues was unaffected by Septin 7 depletion. This was apparent in equivalent up-regulation of c-Myc and CD71 following all forms of stimulation (Fig. 1e,f). Further, *Sept7*KO OT-I cells stimulated by APC-dependent or -independent stimuli up-regulated CD69 and CD25 similarly (Supplementary Fig. 2e,f). Finally, *Sept7*KO OT-I T cell calcium flux in response to anti-CD3 crosslinking or thapsigargin blockade of SERCA uptake was also equivalent to that of wild-type cells (Supplementary Fig. 2g). To determine whether the distinction amongst these stimuli related to strength-of-signal, we co-cultured T cells from control or *Sept7*KO OT-I mice *in vitro* with BMDCs that had been pulsed with peptides differing in pMHC-OT-I-TCR affinity across a range of concentrations and measured CD69 up-regulation after 24 h (Fig. 1g). Weak agonist peptides and lower doses induced less activation by this measure but *Sept7*KO cells behaved identically to controls, demonstrating that *Sept7*KO T cells sensed the density and identity of TCR signals similarly to wild-type cells. Thus, the differences we observed in *Sept7*KO T cell proliferative capacity stimuli did not stem from defective TCR signaling or cell-cycle entry, but rather suggested that APCs contribute key cellular factors that facilitate division of *Sept7*KO T cells.

***Sept7*KO Division Defects with APC-independent Stimuli**

Soluble cytokines also substantially drive T cell expansion and so we tested whether this stimulus would lead to cell division defects in septin-null T cells. We found that naïve septin-deficient CD8⁺ OT-I T cells did not divide *in vitro* following exposure either to homeostatic cytokines IL-7 plus IL-15 or high concentrations of IL-2 (Fig. 2a, Supplementary Fig. 3a)²⁸. Again, defects in *in vitro* proliferation did not appear to result from dysfunctional signaling for *Sept7*KO CD8⁺ OT-I cells phosphorylated STAT5, a target of these cytokine receptors, to a similar extent as control T cells (Fig. 2b). As with TCR-stimulation in the absence of APCs, soluble cytokines induced multi-nucleated septin-deficient CD8⁺ T cells (Fig. 2c). The combination of APC-independent activation (PMA or anti-TCR) with addition of IL-2 also failed to rescue *in vitro* proliferation, suggesting that the defect observed did not result from inadequate cytokine production (Fig. 2d, Supplementary Fig. 3b). Rather, we concluded that, in contrast to stimuli from BMDCs, cytokines alone fail to support cytokinesis of septin-null T cells.

Rescue of Defective Proliferation Through Cell Contacts

We next sought to determine whether BMDCs were providing additional signals that overcame a block in proliferation in *Sept7cKO* cells. To do so, we performed add-back *in vitro* experiments, using PMA and ionomycin as a base stimulus. Addition of peptide-pulsed BMDCs to these OT-I T cell cultures largely restored cell division as assessed by CFSE dilution (Fig. 3a, Supplementary Fig. 4a). This partial rescue was equivalent when BMDCs lacking antigenic peptide were added, demonstrating that BMDCs mediate rescue independently of their ability to generate strong TCR signals. However, supernatant from competent BMDC-T cell cultures, added at 20%, was unable to restore division, suggesting that cell-cell contact was primarily responsible. In addition, we found that resting B cells were unable to support cell division in *Sept7cKO* CD8⁺ OT-I T cells whereas lipopolysaccharide (LPS)-activated B cells facilitated enhanced proliferation (Fig. 3b, Supplementary Fig. 5b), though still not to the same extent as BMDCs (Fig. 1b). That BMDCs and LPS-treated B cells supported *Sept7cKO* OT-I T cell division suggested that this rescue was mediated by cellular properties unique to highly activated APCs.

In addition to TCR signals, APCs provide numerous accessory cues for T cells and we investigated many of these. In doing so, we found that signaling from co-stimulatory molecules to CD28 and from ICAM adhesion molecules to integrin LFA-1 represented a prominent portion of the rescue; antigen-free BMDCs restored cell division to *Sept7cKO* OT-I cells and this was partially inhibited with blocking antibodies to CD80 and CD86 or antibodies to LFA-1 (Fig. 3c, Supplementary Fig. 4b). This block was even more profound when anti-CD80/86 was combined with anti-LFA-1. Surprisingly, blockade mediated by these antibodies was nearly as effective when added 24 h after the initial stimulation with PMA and ionomycin plus BMDCs. This finding suggested that rescue of cell division was mediated by BMDCs in cell-cell contacts that take place well after the initiation of TCR signals.

To test whether these interactions were purely adhesive or resulted from signaling, we repeated the BMDC add-back experiments using several inhibitors that target phosphatidylinositol-3-OH kinase (PI(3)K), a key downstream signal transduction molecule in CD28 and LFA-1 pathways. We found that pan-PI(3)K inhibitor compounds LY294,002 and GDC-0941 blocked the BMDC-mediated rescue of *Sept7cKO* OT-I cell division with a modest reduction in control T cell proliferation (Fig. 3d, Supplementary Fig. 4c). Wild-type cell viability, however, was not grossly impacted at the dose used (data not shown). Notably, blockade of PI(3)K signaling reduced septin-null OT-I T cell proliferation, whether added 24 h after BMDC addition, or at the onset of culture. To extend these findings to a more physiological setting, we similarly inhibited PI(3)K signaling 36 h after co-culturing *Sept7cKO* and control OT-I T cells with SL8-pulsed BMDCs and found that treatment reduced *Sept7cKO* T cell proliferation (Fig. 3e, Supplementary Fig. 4d). Interestingly, control T cell proliferation was again modestly inhibited, with a more substantial loss in proliferation if PI(3)K was inhibited 24 h after initial co-culture with BMDCs (Supplementary Fig. 4e). While the magnitude of this effect was larger for septin-null T cells, this implies that ongoing PI(3)K activity is required for maximal proliferation, even in wild-type T cells.

Consistent with these results, the differential capacity of resting or LPS-treated B cells in facilitating *Sept7cKO* OT-I T cell division was not due to differences in proximal T cell activation as assessed by CD69 up-regulation (Supplementary Fig. 5a). Rather, LPS-treated B cell-driven T cell division was similarly mediated through prolonged signaling via CD28 and LFA-1 and dependent upon PI(3)K (Supplementary Fig. 5b, c). Together these findings support a model whereby APCs establish a niche of cell-cell contact interactions characterized by PI(3)K signaling that complements or compensates for septin function in CD8⁺ T cell division.

Polarized Contacts Support *Sept7cKO* T cell Division

BMDCs bearing CD80, CD86, and ICAM-1 represent a likely polarized surface during cell division and we sought to address whether that feature was sufficient to complement septin deficiency. To address this, we cultured PMA-activated OT-I T cells on wells coated with adhesive molecules including ICAM-1, fibronectin, and antibodies against CD44 and CD28. Of these, ICAM-1 and anti-CD28 were uniquely capable of enhancing septin-null CD8⁺ T cell division (Fig. 4a, Supplementary Fig. 3c). These findings suggest that BMDCs facilitate septin-null division through specific signaling, not merely through general adhesion and cellular contact. Furthermore, by selectively plating OT-I T cells on ICAM-1 at various times during the stimulation, we determined that rescue was taking place at least 24 h after initial activation, but not at the time of initial stimulation (Fig. 4b, Supplementary Fig. 3d). T cells begin dividing at least 24 h after activation⁴ and so this temporal window coincided with the kinetics of T cell entry into the cell cycle and ongoing division.

Septin Dependence Separates Proliferation Drivers *in vivo*

Our *in vitro* findings suggested that the requirement for septins in T cell division distinguishes cell division that is driven by the presence or absence of specific contacts or niches. We therefore compared different activating stimuli *in vivo*. Using the Dec-OVA model of antigen delivery to load antigens onto lymph node resident DCs²⁹ we found that adoptively transferred septin-null CD8⁺ OT-I T cells expanded similarly to their co-transferred wild-type counterparts (Fig. 5a). To test whether *Sept7cKO* T cells continue to require the presence of antigen-loaded APCs after initial activation, CFSE-labeled *Sept7cKO* and control CD8⁺ OT-I T cells were co-cultured *in vitro* with SL8-pulsed BMDCs for 36 h, at which point the T cells were isolated. *Sept7cKO* and control T cells were then re-plated *in vitro* or co-transferred to antigen-free mice. When the T cells were cultured *in vitro*, *Sept7cKO* T cells exhibited notable cell division defects (Fig. 5b, top). *Sept7cKO* T cells, however, were able to divide proficiently compared to control T cells when transferred to antigen-free host mice (Fig. 5b, bottom). These findings suggest that while *Sept7cKO* T cells do not require antigen-bearing APCs during cell division, endogenous interactions *in vivo* that are absent from the T cell-only culture are sufficient to support successful cell division.

In contrast, when anti-IL-2 complexes were delivered to generate cytokine mediated proliferation in the absence of overt APC involvement, expansion of adoptively transferred septin-null OT-I T cells was significantly reduced compared to that of control cells (Fig. 5c). As an additional cytokine-mediated *in vivo* challenge, we transferred polyclonal wild-type

and *Sept7* KO cells into sub-lethally irradiated mice. In these mice, T cells typically undergo a slow form of lymphopenic-induced proliferation, which is thought to mimic an acute form of homeostatic expansion³⁰. Again, septin-null CD8⁺ T cells were impaired in their overall expansion (Fig. 5d). These findings support a context-dependent requirement for septins in T cell division and extend our model to critical *in vivo* processes.

Septin Requirement for CD8⁺ T cell Homeostasis

We found evidence for defects in steady-state homeostatic maintenance of naïve and memory CD8⁺ *Sept7* KO T cells, which is in agreement with findings that Septin 7 is required for cytokine-driven proliferation. Although peripheral CD8 compartments were comparable between *Sept7* KO and control OT-I mice at 6–8 weeks of age, the frequency of CD8⁺ T cells declined after 6 months (Fig. 6a, left, middle). In addition, we found that this was accompanied by a significant loss of phenotypically naïve CD44^{low/med} CD8⁺ T cells in aged *Sept7* KO OT-I mice. Of the CD8⁺ T cells that remained in aged *Sept7* KO mice, CD8⁺ T cells were broadly CD44^{hi} as compared to bimodal expression in control mice (Fig. 6a, right), suggesting a lymphopenic environment in which these surviving *Sept7* KO CD8⁺ T cells may be responding to antigen^{31,32}. Given that memory CD8⁺ T cell homeostasis also relies on cytokines, we examined maintenance of memory CD8⁺ *Sept7* KO T cells. Naïve *Sept7* KO and wild-type CD8⁺ OT-I T cells were co-transferred to host mice that were immunized i.v. with DecOVA. *Sept7* KO T cells were detected 14 days later at similar frequency in the spleen (Fig. 6b, left), although slightly reduced in number in lymph nodes (Supplementary Fig. 6a), and highly expressed memory precursor cell (MPEC) markers CD44 and CD62L (Supplementary Fig. 6b). These *Sept7* KO and wild-type OT-I T cells were then sorted from the spleen and lymph nodes and co-transferred to antigen-free mice. The frequency of *Sept7* KO and control T cells was determined 8 weeks later as previous studies have demonstrated that multiple rounds of homeostatic turnover occurs over this period of time³³. Indeed when quantified, the frequency of *Sept7* KO T cells was significantly lower than control T cells in antigen-free host spleens (Fig. 6b, right), indicating a role for septins in facilitating memory T cell homeostasis. In contrast, while we noted a trend toward preferential wild-type T cell maintenance in the lymph node, it was not as severe as in the spleen (Supplementary Fig. 6c). This observation may speak to intriguingly different milieus between the two organs that support homeostatic division, but remains an area of future investigation. Altogether, this data demonstrates that a lack of septins impedes T cell division in a stimulus-dependent manner *in vivo*.

Discussion

The significance of these results is that we have identified a situation and mechanism that differentiates APC/niche-driven proliferation from niche-independent division. This suggests that specific types of T cell division might be differentially targeted in the future, for example with cytoskeletal inhibitors. This is of particular importance since homeostatic expansion arising from lymphopenic conditions can result in organ transplant rejection or possibly autoimmunity, and is not responsive to co-stimulatory blockade^{34–38}. In fact, a preponderance of clinical immunosuppressive agents are actually directed against antigen-specific T cell expansion, typically targeting pathways downstream of T cell activation such

as mTOR or calcineurin³⁵. Drugs that are available to restrict homeostatic division such as MMF target non-specific processes like DNA synthesis³⁹ that are characteristic of all forms of T cell division, and thus leave patients ill-equipped to face pathogen challenge. Our work suggests that targeting septins and the pathways they use might yield better therapeutic strategies in these cases.

Previous to this work, it had been found that T cells, amongst a select few eukaryotic cells, did not appear to require septins to complete cell division^{17,19}. Now, we understand that the T cell exception reflects, not a cell-type, but a context-dependent role of septins in cell division. In the case of T cells, the context that rescues T cell division is the presence of a highly adhesive and activated surface or cell type. Previous *in vivo* lymph node imaging studies of proliferating T cells demonstrate antigen-specific T cells dividing independently of contact with labeled APCs⁵, though division following DC contact has also been noted⁴⁰. Our findings that APCs or surfaces high in specific co-stimulatory molecules and integrins rescue septin-null T cell cytokinetic defects *in vitro* and *in vivo* provide support that a niche, in which T cells engage in contact interactions during the temporal window of division, serves a functional role. We observed a spectrum of septin-null T cell proliferative competence across the conditions PMA/ionomycin, anti-TCR/anti-CD28, or antigen-pulsed APCs, an effect that thus corresponds to the degree of PI(3)K signaling expected to be generated by these stimuli. It may thus be that a threshold of total PI(3)K signaling must be reached for T cells to divide in the absence of septins. Yet, cytokines like IL-7 and IL-2 generate PI(3)K activity through their receptors as well, and we did not find partial or full rescue of the cytokinesis defect in these conditions. Distinctions in how and when PI(3)K is active likely underlie this, and it is also possible that the activating PI(3)K cue could be counterbalanced by additional cell-cell cues. Based on the data, we favor a model in which APCs can mediate septin-null cell division by providing a highly polarized source of PI(3)K signaling and/or stabilized cell cortex, given at or near the time of cell division.

As septins have been described to establish polarity in yeast and reinforce local membrane compartmentalization by serving as a diffusion barrier^{44,46}, it is tempting to speculate that septins and PI(3)K may cooperate or act redundantly to ensure that proper polarity is maintained while T cells undergo cell division. Notably, compartmentalization of phospholipids has been described as important during cytokinesis as the cytokinetic furrow is enriched for phosphatidylinositol-(4,5)-bisphosphate (PtdIns(4,5)P₂)^{47,48}. While previous studies have found PI(3)K signaling within the first 8 h of T cell activation to be the most critical in impacting eventual proliferation⁴⁹, our data using PI(3)K inhibitors suggests that PI(3)K signaling even 24 h post-T cell activation continue to regulate wild-type T cell proliferative potential and kinetics. Indeed, one area where a dual PI(3)K–septin pharmacological inhibition might prove selective would be in blocking antigen-independent proliferation of leukemic cells while sparing the proliferation of antigen-dependent host T cells.

One surprising result of our data in this paper and previous is that T cell signaling, even at a synapse, is independent of septins. In fact, our original impetus for studying these proteins was that they assemble more densely as a ring around the immune synapse (IS) (J.G. and M.F.K., unpublished). To this extent, our collective data is at odds with recent studies which

used shRNA approaches to implicate septins in efficient STIM1 and ORAI co-localization and subsequent calcium flux in HeLa, Jurkat, and HEK cells^{50,51}. We, in contrast, did not find that differences in septin-deficient T cell division capacity stemmed from defects in TCR signaling processes. One possible reason for this difference would be some form of compensation in our cells for this specific septin function. The presence of cell division defects argues against ubiquitous compensation, and the idea of signaling-specific compensation is not supported by data in which normal calcium flux was observed despite Cre transfection of *Sept7*^{flox/flox} T cell blasts (A.M.M. and M.F.K., unpublished). An alternative explanation for the apparent septin defect reported in cell lines may be that these cells are experiencing cytokinetic failure, and thus defective signaling is relatively distal to septin deficiency. At present, although we cannot support that there is a requirement of septins for T cell calcium signaling, further work may be needed to determine how and when our findings align with previous signaling studies.

Why were we ever able to isolate T cells from the periphery of conditional knockout mice if cell division is possibly compromised? One answer is that while the *Cd4*-Cre allele depletes septins in the pre-DP window, T cells post-DP stage typically do not divide again unless called upon to do so for homeostatic expansion. Additionally, with respect to homeostatic processes, although septin-null cells are clearly defective in expanding *in vivo* when transferred to a sub-lethally irradiated mouse, the effect was not as profound as the division defect to pure cytokines *in vitro*. It may be that some maintenance, if not expansion, of T cells in developing mice can involve synaptic cell-cell encounters that are septin-independent. For example, IL-15 is trans-presented to CD8⁺ T cells by another cell bearing the alpha chain⁵². Additionally, T cells at steady-state engage in cellular contact with APCs presenting self-pMHC and/or fibroblastic reticular cells (FRCs) that produce homeostatic cytokines like IL-7⁷.

What is the breadth of this requirement? Septin-null T cells did appear to selectively lose CD44⁻CD8⁺ populations in lymph nodes^{31,32} and we also observed defective homeostasis of memory CD8⁺ OT-I *Sept7* KO T cells in the spleen. In light of the trend in septin requirement, these findings suggest that endogenous cell-cell contacts in these settings do not mediate *Sept7* KO T cell division like endogenous cell-cell contacts do for activated T cells. Although we found no specific defects in septin-deficient T cells for effector generation as assessed by surface markers or interferon- γ at day 6 post-immunization (A.M.M, J.G. and M.F.K., unpublished), late-stage cellular contacts such as those during asymmetric cell division or in late-stage T-T interactions^{8,41} may supply an additional higher degree of complexity in T cell effector and memory development, as well as clonal burst size and sustained survival. In sum, septin-dependent versus -independent immune cell cytokinesis indicates the possibilities for enhanced selective targeting of proliferative processes.

Methods

Mice

Sept7 KO *Sept7*^{flox/flox} mice¹⁹ were crossed to *Cd4*-Cre transgenic mice²⁷ to deplete Septin 7 in T cells. These mice were bred to Ovalbumin (OVA)-specific TCR transgenic OT-I

mice⁵³ and/or mTmG mice²⁶ (The Jackson Laboratory). Cells designated as experimental controls were generated from *Sept7^{fllox/fllox} Cd4-Cre⁻* or *Sept7^{fllox/-} Cd4-Cre⁺* mice. These mice, along with C57BL/6 (The Jackson Laboratory and Simonsen) and CD45.1⁺ mice, were housed and bred under specific pathogen-free conditions at the University of California Animal Barrier Facility. All experiments using mice were approved by the Institutional Animal Care and Use Committee of the University of California.

Cell isolation

CD8⁺ polyclonal or OT-I T cells were isolated from lymph nodes of 6–8-week-old mice using EasySep CD8 negative selection kits (STEMCELL Technologies). B cells were isolated from spleens of 6–8-week-old mice using EasySep B cell negative selection kits (STEMCELL Technologies). In specified experiments, B cells were treated with 1 µg/ml LPS (Sigma-Aldrich) for 5 h before use. BMDCs were generated from treating cultured bone marrow cells with GM-CSF (granulocyte-macrophage colony-stimulating factor) for 7–11 days. IL-4 was added for the last 2 days with 1 µg/ml LPS stimulation 6–24 h before use. BMDCs and B cells were incubated with 1–100 ng/ml SL8 OVA peptide (SIINFEKL) (Anaspec), or variant peptides N4, T4, Q4H7, V4 (gift from E. Palmer and D. Zehn) for at least 30 min at 37°C and washed 3 times.

Immunoblot

Naïve CD8⁺ T cells were isolated from 6 week-old *Sept7*CKO and littermate control OT-I mice. 10⁶ cells per sample were lysed in PBS containing 1% Triton X-100 in the presence of a cocktail of protease and phosphatase inhibitors (2 µg/ml aprotinin, 2 µg/ml leupeptin, 2 mM phenylmethyl sulfonyl fluoride (PMSF), 10 mM sodium fluoride, 10 mM iodoacetamide and 1 mM sodium orthovanadate). After 15 min lysis on ice, lysates were spun at high speed for 10 min to remove insoluble material and protein concentration in the supernatant was quantified by the Bio-Rad detergent-compatible protein assay to ensure equal loading. Samples were resolved by SDS-PAGE, and immunoblot analysis was performed using rabbit polyclonal primary antibodies against Sept1, Sept6C, Sept9⁵⁴, Sept7 (IBL-America, Inc.), and HRP-Conjugated Goat anti-Rabbit secondary antibody (Jackson ImmunoResearch) Relative protein abundance was quantified using ImageJ software (NIH). Cell number ($\times 10^3$)

In vitro T cell activation assays

Isolated T cells were labeled with 0.5–5 µM CFSE (carboxyfluorescein diacetate succinimidyl ester; Invitrogen) or CellTrace Proliferation Dye (BD Biosciences) for 15 min at 37 °C, cultured in 96-well plates at a density of 0.1×10^6 /ml in complete RPMI and harvested for analysis 72 h later unless noted otherwise. CD8⁺ T cells were cultured on plate-bound anti-CD3 (2C11; UCSF Hybridoma Core) or anti-TCRβ (H57-597; produced in our lab) with addition of soluble anti-CD28 at 2 µg/ml (PV-1; UCSF Hybridoma Core). Alternatively, T cells were stimulated with 100–1000 ng/ml PMA (phorbol 12-myristate 13-acetate) and 125 ng/ml ionomycin. In specified experiments 10–20 U/ml of recombinant human IL-2 (NIH AIDS Reagent Program) or 20% supernatant harvested from previous wild-type BMDC-T cell cultures was added at time of plating. For other indicated experiments, 96-well plates were coated with the following antibodies or proteins: 10 µg/ml

anti-CD44 (IM7, eBiosciences), 10 µg/ml anti-CD28 (PV-1; UCSF Hybridoma Core), 5 µg/ml recombinant mouse ICAM-1 Fc Chimera protein (R&D Systems), or 10 µg/ml fibronectin, bovine plasma (EMD Millipore). In some experiments, cells were moved to or removed from plates containing ICAM-1 Fc Chimera protein, prepared as detailed above.

In co-culture experiments, OT-I T cells were plated with activated BMDCs at a 10:1 ratio in flat-bottom wells, or with isolated B cells at a 1:1 ratio in round-bottom wells. In specified experiments, 10 µM of PI(3)K inhibitors LY-294,002 (Sigma-Aldrich) or GDC-0941 (gift from J. Roose) was added to culture 24 h or 36 h after plating. For BMDC rescue assays, T cells were stimulated with PMA and ionomycin, and mature activated BMDCs were added at time of plating. To block co-stimulatory signaling, 10 µg/ml anti-CD80 (16-10A1; UCSF Hybridoma Core) and 10 µg/ml anti-CD86 (GL-1; UCSF Hybridoma Core) and/or anti-CD11a (M17/4; UCSF Hybridoma Core) was added to culture 0 or 24 h after plating. Alternatively, 10 µM of LY-294,002 or 10 µM GDC-0941 was added 0 or 24 h after plating. In other experiments, T cells were plated with activated BMDCs at a 5:1 ratio, isolated with a CD8 negative selection kit, and re-plated with 10 U/ml of human recombinant IL-2.

Cytokine exposure

Isolated CD8⁺ OT-I T cells were cultured in 96-well plates at a density of 0.1×10^6 /ml. 5000 U/ml of human recombinant IL-2, or murine recombinant 5 ng/ml IL-7 (Peprotech) and 100 ng/ml IL-15 (Peprotech) were added to media at time of plating, with cells harvested for analysis 5 days later.

Surface and intracellular flow cytometry staining

Cells were harvested from lymph nodes, spleens, or *in vitro* culture, washed with PBS and non-specific binding blocked with flow cytometry buffer (PBS, 2% FCS) and anti-CD16/32 (2.4G2; UCSF Hybridoma Core). Surface proteins on cells were stained with the following antibodies for 25 min at 4 °C: anti-CD69 (H1.2F3; eBiosciences), anti-CD25 (PC61.5; eBiosciences), anti-CD71 (C2, BD Pharmingen), anti-CD8α (53-6.7 eBiosciences), anti-CD4 (RM4-5; BioLegend), anti-CD44 (IM7; eBiosciences), anti-CD45.1(A20; eBiosciences), or anti-CD45.2 (104; BioLegend). Cells were again washed and resuspended with flow cytometry buffer before data collection, with addition of black latex beads to samples to quantify cellular number.

For intracellular stains, cells were washed with PBS, incubated with Zombie NIR fixable viability dye (BioLegend) at 4 °C for 30 min to demarcate dead cells. Cells were next washed and fixed with 4% PFA for 15 min at 20 °C. Lastly, cells were washed and stained in flow cytometry buffer with 0.2% saponin, along with anti-Septin 7⁵⁴ or phalloidin probe (Invitrogen) for 30 min before a final wash and resuspension in flow cytometry buffer. Alternatively, fixed cells were treated with cold (−20°C) MeOH for 30 min at 4°C. Cells were then stained for 1 h at 20 °C in staining buffer (PBS, 1% BSA) containing anti-c-Myc (D84C12; Cell Signaling Technology), washed, and stained with fluorescently labeled donkey F(ab')₂ anti-rabbit (Abcam) for 30 min at 20 °C.

For assessing cellular DNA content with Hoechst dye, harvested cells were washed with PBS, fixed in 70% EtOH for 30 min on ice, and washed twice again with PBS. Cells were

then incubated with PBS containing 0.1% Triton-X-100, 0.1 mM EDTA, 100 µg/ml RNase A (Thermo Scientific), and 5 µg/ml Hoechst dye (Thermo Scientific). Cells were again washed and resuspended in flow cytometry buffer.

STAT5 phosphorylation assay

Isolated CD8⁺ OT-I T cells were cultured in 96-well plates and activated through PMA and ionomycin stimulation or co-culture with SL8-pulsed activated BMDCs. Anti-mouse IL-2 (15 µg/ml, JES6-1A12) was added to cultures at time of plating to restrict IL-2 delivery. After 24 h, recombinant human IL-2 (0.1–100 U/ml) was added to wells for 20 min at 37 °C. Cells were washed, fixed with 4% PFA for 15 min at 20 °C, and washed. Cells were resuspended with cold (–20 °C) MeOH and washed with flow cytometry buffer 4 times. To stain, cells were incubated in PBS containing 2% BSA and anti-phospho-STAT5 (C71E5; Cell Signaling Technology) before a final wash and resuspension in flow cytometry buffer.

Calcium flux signaling

Isolated CD8⁺ OT-I cells were labeled with 1 µM ratiomeric calcium-binding dye Indo-1, AM (Life Technologies) in PBS for 15 min at 37 °C. Cells were washed twice with complete RPMI, and incubated at 37 °C for 15 min to allow for complete de-esterification. Cells were coated with 5 µg/ml anti-CD3 (2C11; UCSF Hybridoma Core) on ice, washed, and transferred to 37 °C 10 min prior to data collection. To induce CD3 cross-linking, 10 µg/ml of anti-Armenian hamster (BioLegend) was added to CD3-coated cells after 1 min of sample collection. Alternatively, 1 µM of thapsigargin (Sigma-Aldrich) was added to uncoated cells. Cell samples were kept in a heating chamber (37 °C) during data collection by flow cytometry.

In vivo cell transfer and Dec-OVA immunization

Isolated CD8⁺ T cells were resuspended in PBS and adoptively transferred by retro-orbital or tail-vein injection to recipient mice. 0.5×10^6 CFSE-labeled wild-type and *Sept7*KO polyclonal T cells were co-transferred to host mice that had been sub-lethally irradiated. Inguinal lymph nodes and spleen were harvested and analyzed 14 days following transfer. $0.5\text{--}1 \times 10^6$ CFSE-labeled wild-type and *Sept7*KO CD8⁺ OT-I T cells that had been co-cultured *in vitro* with SL8-pulsed BMDCs were isolated and co-transferred to antigen-free host mice. Spleens were harvested and analyzed 48 h later. Alternatively, 2.5×10^3 wild-type and *Sept7*KO OT-I T cells were co-transferred to congenic wild-type mice, respectively. Dec-OVA complexes were generated in-house from conjugation of anti-Dec205 (NLDC-145) to OVA. 1 µg of Dec-OVA, along with 10 µg of anti-CD40 (1C10; eBiosciences), was injected subcutaneously in the left and right flanks of host mice. Inguinal lymph nodes were harvested and analyzed 6 or 7 days later.

For memory homeostasis experiments, 2.5×10^6 naïve CD8⁺ OT-I wild-type and *Sept7*KO T cells were co-transferred to host mice that were immunized i.v. with 10 µg DecOVA and 50 µg anti-CD40. Transferred T cells were sorted from pooled spleens and lymph nodes of these mice 14 days later, counted, and $0.5\text{--}1 \times 10^6$ wild-type and *Sept7*KO cells were co-transferred to antigen-free mice. Spleens and lymph nodes were harvested and analyzed 8 weeks later.

***In vivo* cell transfer and IL-2 complex delivery**

1×10^6 isolated *Sept7* KO or control OT-I CD8⁺ T cells were adoptively transferred by retro-orbital injection to congenic recipient mice. IL-2 complexes were formed by incubating 1 μ g of recombinant murine IL-2 peptide (Peprotech) with 5 μ g murine anti-IL-2 (S4B6-1; BioXCell) for 1 h at 20 °C. PBS was added and the solution administered by intraperitoneal injections. IL-2 complexes were freshly made and injected daily, with harvesting and analysis of inguinal lymph nodes and spleen after 7 days.

T cell morphology analysis

T cells were activated, and imaged on ICAM-coated coverslips with 0.25% low-melt agarose for morphological analysis. Cell length was measured using Metamorph software's *Integrated Morphometry Analysis* (IMA) measurement tool. Images were acquired on a modified Zeiss Axiovert 200M microscope with a plan-neofluor 63 \times objective (Carl Zeiss) using Metamorph imaging software (MDS Analytical Tech).

Confocal microscopy

Isolated CD8⁺ T cells were stimulated with PMA and ionomycin, and cultured for 48 h. Cells were then transferred to poly-L-Lysine coated chamber slides. Once adherent, cells were washed twice with PBS, fixed with 4% PFA (PBS) for 15 min at 20 °C and washed. Cells were permeabilized with 0.1% Triton-X-100 (PBS) for 5 min, and washed twice with 1% BSA (PBS). Cells were then stained with DAPI (Invitrogen) before a final wash and application of a cover slip. Images of cells were generated using an inverted Yokogawa CSU-10 spinning-disk confocal microscope (Zeiss) with Micro-Manager imaging software (www.micro-manager.org).

CFSE quantification

A mean CFSE peak number was quantified for each *in vitro* proliferation experiment with CFSE-labeled T cells. For a given sample's CFSE profile of live cells, each CFSE peak was gated, and the percentage of cells populating the peak was generated. A weighted mean of the number of CFSE peaks diluted was then calculated.

Statistics

Comparisons between groups were analyzed with Student's *t*-test as indicated with GraphPrism software. Data was denoted as significant if *P*-values were 0.05 or less.

Supplementary Material

Refer to Web version on PubMed Central for supplementary material.

Acknowledgments

We thank the Biological Imaging Development Center personnel (UCSF) for technical assistance with imaging, J. Roose and O. Ksionda (UCSF) for reagents and helpful discussion, E. Palmer (University Hospital Basel and University of Basel) and D. Zehn (Swiss Vaccine Research Institute and Lausanne University Hospital) for reagents, and M. Kuhns (University of Arizona College of Medicine) for critical reading of the manuscript. This work was supported by NIH R01AI52116 (M.F.K).

References

1. Hogquist KA, Jameson SC. The self-obsession of T cells: how TCR signaling thresholds affect fate 'decisions' and effector function. *Nat Immunol.* 2014; 15:815–823. [PubMed: 25137456]
2. Murali-Krishna K, et al. In vivo dynamics of anti-viral CD8 T cell responses to different epitopes. An evaluation of bystander activation in primary and secondary responses to viral infection. *Adv Exp Med Biol.* 1998; 452:123–142. [PubMed: 9889966]
3. Zehn D, Lee SY, Bevan MJ. Complete but curtailed T-cell response to very low-affinity antigen. *Nature.* 2009; 458:211–214. [PubMed: 19182777]
4. Mempel TR, Henrickson SE, von Andrian UH. T-cell priming by dendritic cells in lymph nodes occurs in three distinct phases. *Nature.* 2004; 427:154–159. [PubMed: 14712275]
5. Miller MJ, Safrina O, Parker I, Cahalan MD. Imaging the single cell dynamics of CD4+ T cell activation by dendritic cells in lymph nodes. *J Exp Med.* 2004; 200:847–856. [PubMed: 15466619]
6. Ehl S, Hombach J, Aichele P, Hengartner H, Zinkernagel RM. Bystander activation of cytotoxic T cells: studies on the mechanism and evaluation of in vivo significance in a transgenic mouse model. *J Exp Med.* 1997; 185:1241–1251. [PubMed: 9104811]
7. Takada K, Jameson SC. Naive T cell homeostasis: from awareness of space to a sense of place. *Nat Rev Immunol.* 2009; 9:823–832. [PubMed: 19935802]
8. Chang JT, et al. Asymmetric T lymphocyte division in the initiation of adaptive immune responses. *Science.* 2007; 315:1687–1691. [PubMed: 17332376]
9. Nigg EA. Mitotic kinases as regulators of cell division and its checkpoints. *Nat Rev Mol Cell Biol.* 2001; 2:21–32. [PubMed: 11413462]
10. Oh Y, Bi E. Septin structure and function in yeast and beyond. *Trends Cell Biol.* 2011; 21:141–148. [PubMed: 21177106]
11. Surka MC, Tsang CW, Trimble WS. The mammalian septin MSF localizes with microtubules and is required for completion of cytokinesis. *Mol Biol Cell.* 2002; 13:3532–3545. [PubMed: 12388755]
12. Estey MP, Di Ciano-Oliveira C, Froese CD, Bejide MT, Trimble WS. Distinct roles of septins in cytokinesis: SEPT9 mediates midbody abscission. *J Cell Biol.* 2010; 191:741–749. [PubMed: 21059847]
13. Estey MP, et al. Mitotic regulation of SEPT9 protein by cyclin-dependent kinase 1 (Cdk1) and Pin1 protein is important for the completion of cytokinesis. *J Biol Chem.* 2013; 288:30075–30086. [PubMed: 23990466]
14. Kinoshita M, Field CM, Coughlin ML, Straight AF, Mitchison TJ. Self- and actin-templated assembly of mammalian septins. *Dev Cell.* 2002; 3:791–802. [PubMed: 12479805]
15. Kinoshita M. Assembly of mammalian septins. *J Biochem.* 2003; 134:491–496. [PubMed: 14607974]
16. Rodal AA, Kozubowski L, Goode BL, Drubin DG, Hartwig JH. Actin and septin ultrastructures at the budding yeast cell cortex. *Mol Biol Cell.* 2005; 16:372–384. [PubMed: 15525671]
17. Tooley AJ, et al. Amoeboid T lymphocytes require the septin cytoskeleton for cortical integrity and persistent motility. *Nat Cell Biol.* 2009; 11:17–26. [PubMed: 19043408]
18. Ageta-Ishihara N, et al. Septins promote dendrite and axon development by negatively regulating microtubule stability via HDAC6-mediated deacetylation. *Nat Commun.* 2013; 4:2532. [PubMed: 24113571]
19. Menon MB, et al. Genetic deletion of SEPT7 reveals a cell type-specific role of septins in microtubule destabilization for the completion of cytokinesis. *PLoS Genet.* 2014; 10:e1004558. [PubMed: 25122120]
20. Hartwell LH. Genetic control of the cell division cycle in yeast. IV Genes controlling bud emergence and cytokinesis. *Exp Cell Res.* 1971; 69:265–276. [PubMed: 4950437]
21. Mostow S, Cossart P. Septins: the fourth component of the cytoskeleton. *Nat Rev Mol Cell Biol.* 2012; 13:183–194. [PubMed: 22314400]
22. Gilden JK, Peck S, Chen YC, Krummel MF. The septin cytoskeleton facilitates membrane retraction during motility and blebbing. *J Cell Biol.* 2012; 196:103–114. [PubMed: 22232702]

23. Joo E, Surka MC, Trimble WS. Mammalian SEPT2 Is Required for Scaffolding Nonmuscle Myosin II and Its Kinases. *Dev Cell*. 2007; 13:677–690. [PubMed: 17981136]
24. El Amine N, Kechad A, Jananji S, Hickson GRX. Opposing actions of septins and Sticky on Anillin promote the transition from contractile to midbody ring. *J Cell Biol*. 2013; 203:487–504. [PubMed: 24217622]
25. Kechad A, Jananji S, Ruella Y, Hickson GRX. Anillin Acts as a Bifunctional Linker Coordinating Midbody Ring Biogenesis during Cytokinesis. *Curr Biol*. 2012; 22:197–203. [PubMed: 22226749]
26. Muzumdar MD, Tasic B, Miyamichi K, Li L, Luo L. A global double-fluorescent Cre reporter mouse. *Genesis*. 2007; 45:593–605. [PubMed: 17868096]
27. Lee PP, et al. A critical role for Dnmt1 and DNA methylation in T cell development, function, and survival. *Immunity*. 2001; 15:763–774. [PubMed: 11728338]
28. Cho JH, et al. Unique features of naive CD8+ T cell activation by IL-2. *J Immunol*. 2013; 191:5559–5573. [PubMed: 24166977]
29. Bonifaz LC, et al. In vivo targeting of antigens to maturing dendritic cells via the DEC-205 receptor improves T cell vaccination. *J Exp Med*. 2004; 199:815–824. [PubMed: 15024047]
30. Sprent CDSJ. Homeostasis of Naive and Memory T Cells. *Immunity*. 2008; 29:848–862. [PubMed: 19100699]
31. Kieper WC, Jameson SC. Homeostatic expansion and phenotypic conversion of naive T cells in response to self peptide/MHC ligands. *Proc Natl Acad Sci USA*. 1999; 96:13306–13311. [PubMed: 10557316]
32. Sprent J, Surh CD. Normal T cell homeostasis: the conversion of naive cells into memory-phenotype cells. *Nat Immunol*. 2011; 12:478–484. [PubMed: 21739670]
33. Choo DK, Murali-Krishna K, Anita R, Ahmed R. Homeostatic turnover of virus-specific memory CD8 T cells occurs stochastically and is independent of CD4 T cell help. *J Immunol*. 2010; 185:3436–3444. [PubMed: 20733203]
34. Wu Z, et al. Homeostatic proliferation is a barrier to transplantation tolerance. *Nat Med*. 2004; 10:87–92. [PubMed: 14647496]
35. Monti P, Piemonti L. Homeostatic T cell proliferation after islet transplantation. *Clin Dev Immunol*. 2013; 2013:217934. [PubMed: 23970924]
36. Khoruts A, Fraser JM. A causal link between lymphopenia and autoimmunity. *Immunol Lett*. 2005; 98:23–31. [PubMed: 15790505]
37. Gattinoni L, et al. Removal of homeostatic cytokine sinks by lymphodepletion enhances the efficacy of adoptively transferred tumor-specific CD8+ T cells. *J Exp Med*. 2005; 202:907–912. [PubMed: 16203864]
38. Tchao NK, Turka LA. Lymphodepletion and homeostatic proliferation: implications for transplantation. *Am J Transplant*. 2012; 12:1079–1090. [PubMed: 22420320]
39. Kitchin JE, Pomeranz MK, Pak G, Washenik K, Shupack JL. Rediscovering mycophenolic acid: a review of its mechanism, side effects, and potential uses. *J Am Acad Dermatol*. 1997; 37:445–449. [PubMed: 9308561]
40. Stoll S, Delon J, Brotz TM, Germain RN. Dynamic imaging of T cell-dendritic cell interactions in lymph nodes. *Science*. 2002; 296:1873–1876. [PubMed: 12052961]
41. Gérard A, et al. Secondary T cell-T cell synaptic interactions drive the differentiation of protective CD8+ T cells. *Nat Immunol*. 2013; 14:356–363. [PubMed: 23475183]
42. Zang JH, et al. On the role of myosin-II in cytokinesis: division of Dictyostelium cells under adhesive and nonadhesive conditions. *Mol Biol Cell*. 1997; 8:2617–2629. [PubMed: 9398680]
43. Fooksman DR, et al. Functional anatomy of T cell activation and synapse formation. *Annu Rev Immunol*. 2010; 28:79–105. [PubMed: 19968559]
44. Barral Y, Mermall V, Mooseker MS, Snyder M. Compartmentalization of the cell cortex by septins is required for maintenance of cell polarity in yeast. *Mol Cell*. 2000; 5:841–851. [PubMed: 10882120]
45. Caudron F, Barral Y. Septins and the lateral compartmentalization of eukaryotic membranes. *Dev Cell*. 2009; 16:493–506. [PubMed: 19386259]

46. Saarikangas J, Barral Y. The emerging functions of septins in metazoans. *EMBO J.* 2011; 12:1118–1126.
47. Field SJ, et al. PtdIns(4,5)P2 functions at the cleavage furrow during cytokinesis. *Curr Biol.* 2005; 15:1407–1412. [PubMed: 16085494]
48. Janetopoulos C, Devreotes P. Phosphoinositide signaling plays a key role in cytokinesis. *J Cell Biol.* 2006; 174:485–490. [PubMed: 16908667]
49. Costello PS, Gallagher M, Cantrell DA. Sustained and dynamic inositol lipid metabolism inside and outside the immunological synapse. *Nat Immunol.* 2002; 3:1082–1089. [PubMed: 12389042]
50. Sharma S, et al. An siRNA screen for NFAT activation identifies septins as coordinators of store-operated Ca²⁺ entry. *Nature.* 2014; 499:238–242. [PubMed: 23792561]
51. Maléth J, Choi S, Muallem S, Ahuja M. Translocation between PI(4,5)P2-poor and PI(4,5)P2-rich microdomains during store depletion determines STIM1 conformation and Orai1 gating. *Nat Commun.* 2014; 5:5843. [PubMed: 25517631]
52. Dubois S, Mariner J, Waldmann TA, Tagaya Y. IL-15R α recycles and presents IL-15 In trans to neighboring cells. *Immunity.* 2002; 17:537–547. [PubMed: 12433361]
53. Hogquist KA, et al. T cell receptor antagonist peptides induce positive selection. *Cell.* 1994; 76:17–27. [PubMed: 8287475]
54. Ihara M, et al. Cortical organization by the septin cytoskeleton is essential for structural and mechanical integrity of mammalian spermatozoa. *Dev Cell.* 2005; 8:343–52. [PubMed: 15737930]

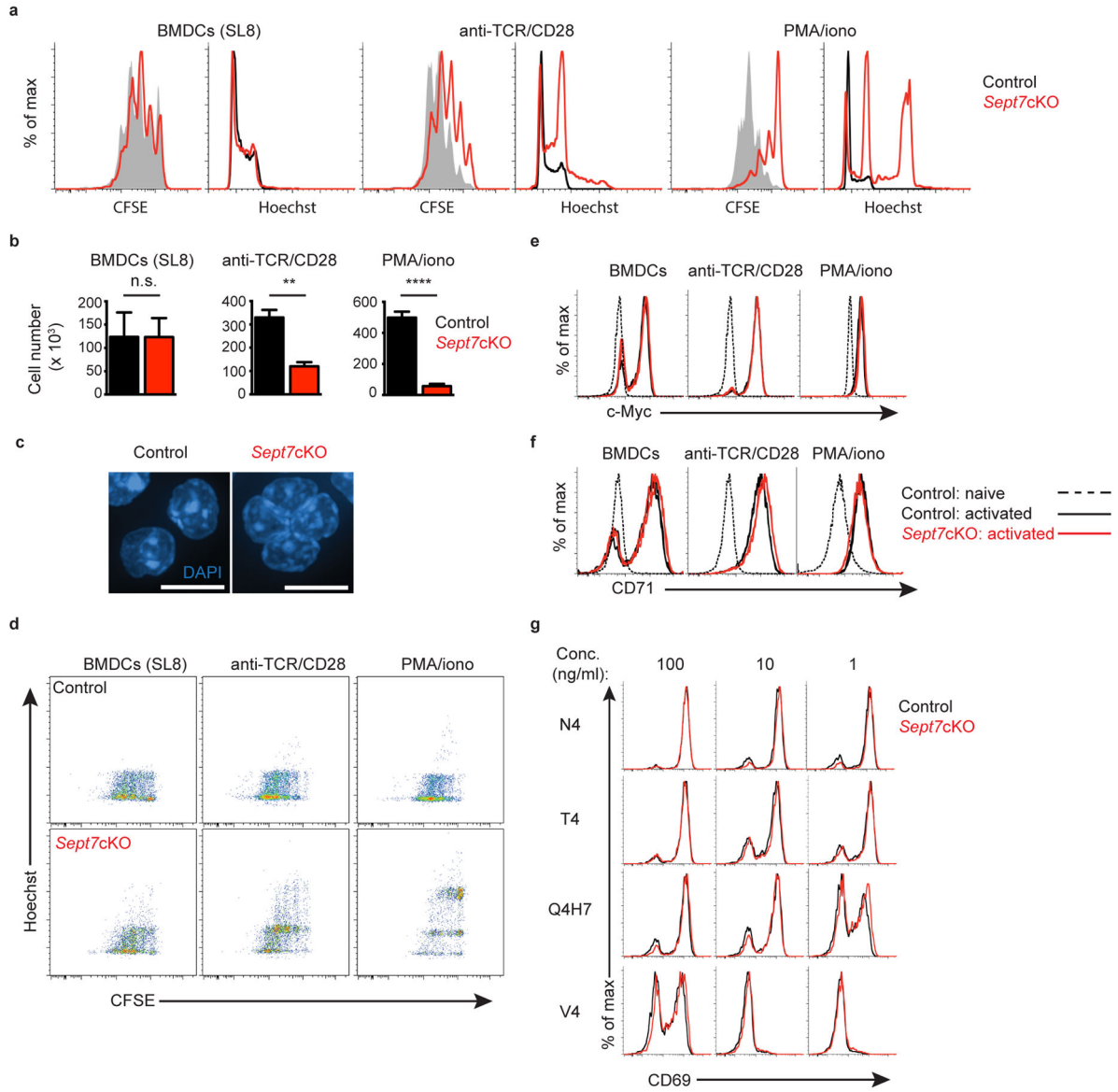


Figure 1. Septin-deficient T cells exhibit selective cytokinetic defects upon APC-independent stimulation

(a–b) *Sept7cKO* and control CD8⁺ OT-I T cells were activated *in vitro* through co-culture with SL8-pulsed (100ng/ml) BMDCs, culture on plate-bound anti-TCR and soluble anti-CD28, or stimulation with PMA and ionomycin. Proliferation and cellular DNA content of live blasted cells were assessed by flow cytometry 72h later as indicated by CFSE dilution and Hoechst, respectively (a), along with cell number recovery (b). (c) Confocal images of fixed *Sept7cKO* and control CD8⁺ polyclonal T cell nuclei stained with DAPI 48h after activation with PMA and ionomycin. Scale bar, 10µM. (d) Kinetics of OT-I multinucleation formation through comparison of CFSE and Hoechst content by flow cytometry 72h following a given activation condition. (e, f) Intracellular expression of c-myc (e) and cell surface expression of CD71 (f) expressed in naïve or activated live *Sept7cKO* and control CD8⁺ OT-I T cells 24h after activation. (g) Cell surface CD69 levels expressed by live

*Sept7c*KO and control CD8⁺ OT-I T cells 24h after co-culture with BMDCs pulsed with a given OT-I peptide and concentration. Small horizontal lines denote the standard error of the mean (SEM). Data is representative of at least two (**c**) or three (**a, d–g**) independent experiments or pooled from the average values of technical triplicates from three independent experiments (**b**). *P < 0.05, **P < 0.01, ***P < 0.001, ****P < 0.0001 with data analyzed with unpaired *t*-test (**b**).

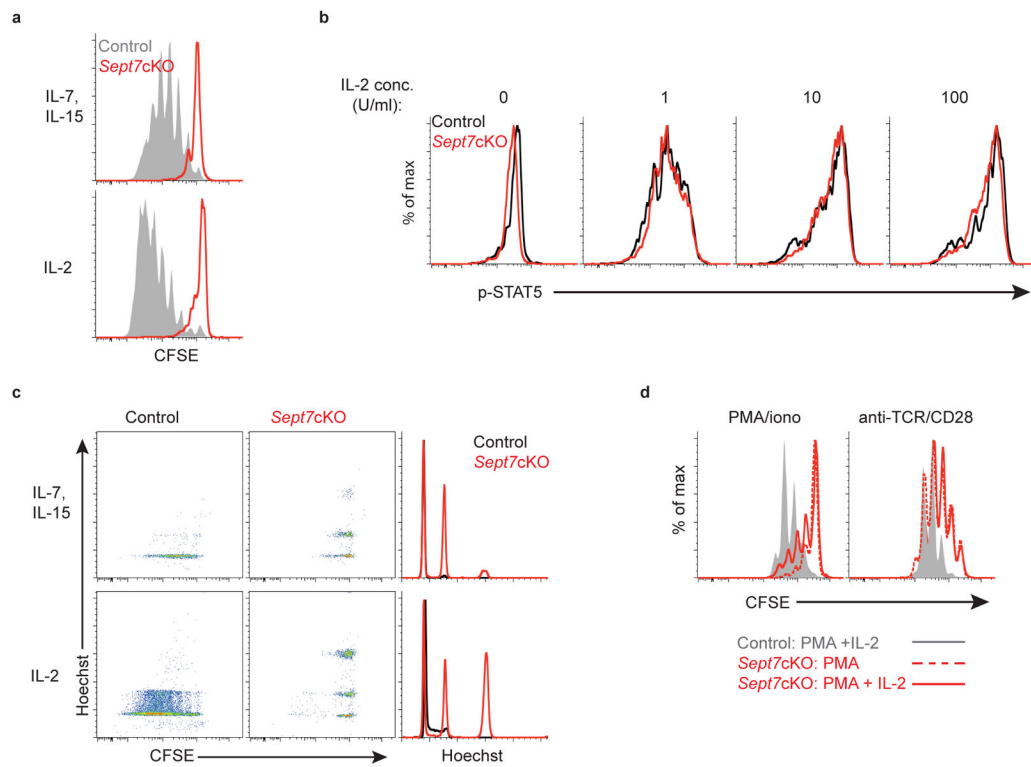


Figure 2. Septin-deficient T cells undergo cytokinetic failure following cytokine exposure
(a) Proliferation as indicated by CFSE dilution of live naïve *Sept7cKO* and control CD8⁺ OT-I T cells following *in vitro* culture with IL-7 (5ng/ml) and IL-15 (100ng/ml) (**top**), or IL-2 (5000U/ml) (**bottom**) for 5 days. **(b)** Intracellular levels of phosphorylated STAT5 in live control and *Sept7cKO* CD8⁺ OT-I T cells following IL-2 exposure 24h after cells were stimulated with PMA and ionomycin. **(c)** CFSE dilution and Hoechst levels in live *Sept7cKO* and control CD8⁺ OT-I T cells cultured *in vitro* with IL-7 and IL-15 (**top**) or IL-2 (**bottom**). **(d)** Proliferation of live *Sept7cKO* and control CD8⁺ OT-I T cells 72h following *in vitro* activation as indicated with addition of IL-2 (10–20 U/ml) at initial plating. Data is representative of at least three independent experiments.

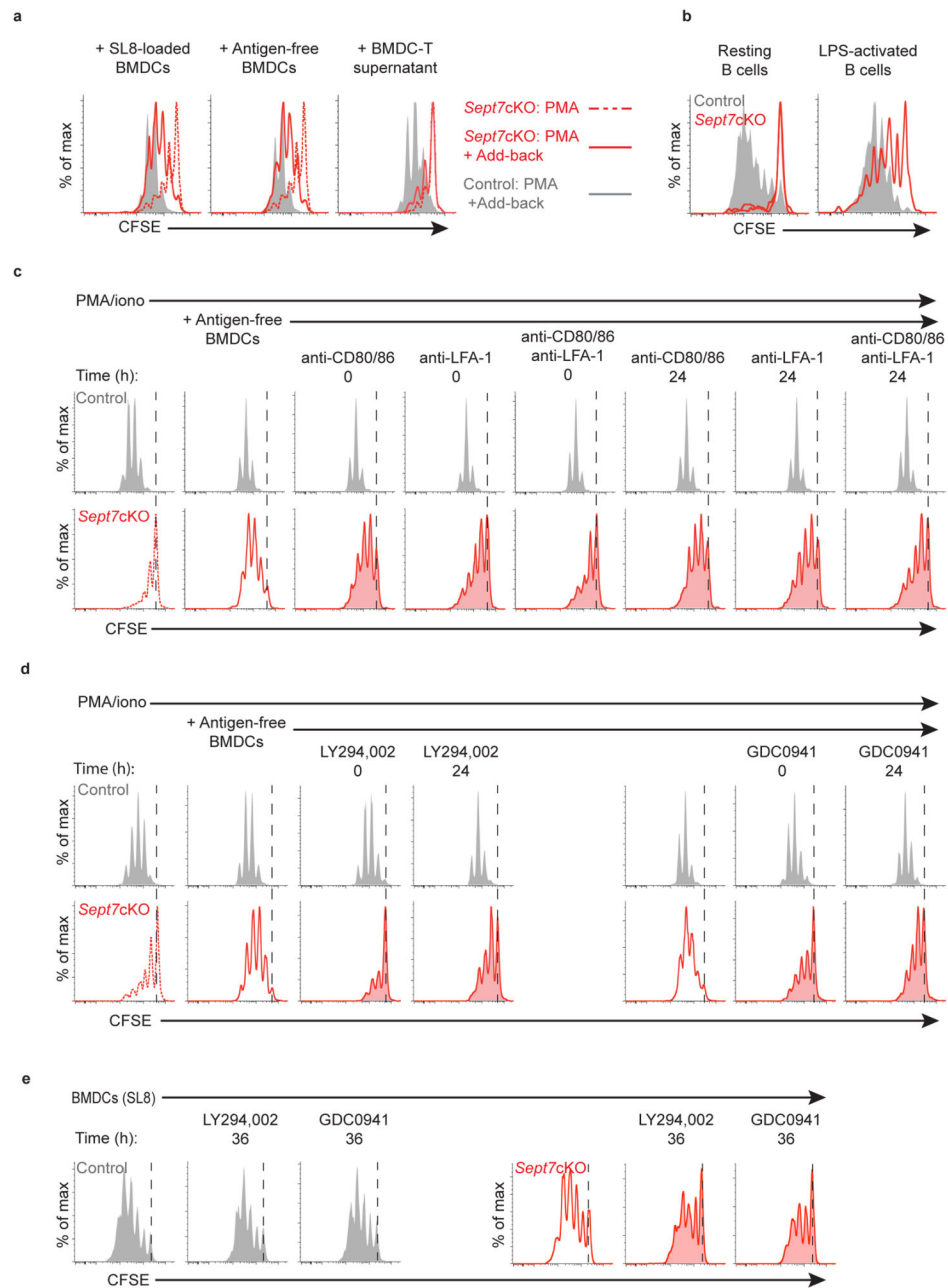


Figure 3. APCs mediate rescue of septin-null CD8⁺ T cell cytokinetic defect through co-stimulatory PI(3)K signaling

(a) CFSE dilution of live *Sept7cKO* or control CD8⁺ OT-I T cells stimulated with PMA and ionomycin and co-cultured at the time of plating with SL8-pulsed (100ng/ml) BMDCs (left), unpulsed BMDCs (middle), or 20% supernatant generated from wild-type BMDC-T cell cultures (right). (b) CFSE dilution of live *Sept7cKO* or control CD8⁺ OT-I T cells following 72h of co-culture with resting or LPS-treated SL8-pulsed splenic B cells. (c, d) CFSE dilution of live *Sept7cKO* or control CD8⁺ OT-I T cells that were stimulated with PMA and ionomycin, co-cultured with unpulsed BMDCs, and subsequently treated with blocking

antibodies against CD80, CD86, and/or LFA-1 (**c**), or PI(3)K inhibitors LY294,002 (10 μ M) or GDC-0941 (10 μ M) (**d**) at the designated time after initial plating. (**e**) CFSE dilution of *Sept7*cKO or control CD8+ OT-I live blasted T cells that were co-cultured with SL8-pulsed (1–100ng/ml) BMDCs and treated with PI(3)K inhibitors LY294,002 (10 μ M) or GDC-0941 (10 μ M) 36h after plating. Data is representative of at least three (**a, e**), four (**b**), or five (**c, d**) independent experiments.

Author Manuscript

Author Manuscript

Author Manuscript

Author Manuscript

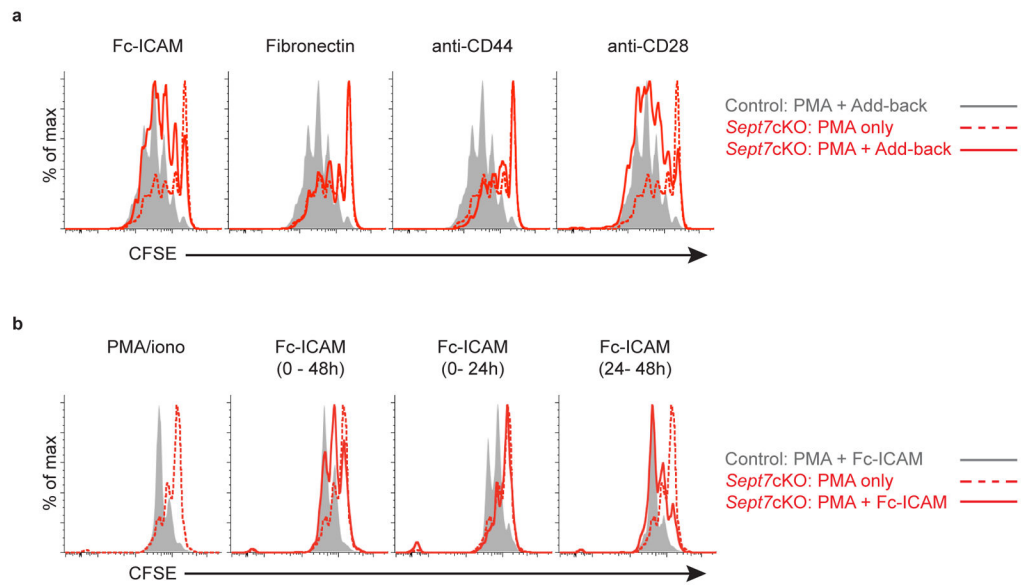


Figure 4. Co-stimulatory signaling is sufficient to enhance septin-null CD8⁺ T cell division

(a) CFSE dilution of live *Sept7cKO* or control CD8⁺ OT-I T cells stimulated with PMA and ionomycin and cultured on plate-bound Fc-ICAM, fibronectin, anti-CD44, or anti-CD28 for 72h. (b) CFSE dilution of live *Sept7cKO* or control CD8⁺ OT-I T cells stimulated with PMA and ionomycin for 48h and cultured on plate-bound Fc-ICAM for a designated interval of time following initial plating. Data is representative of at least three independent experiments.

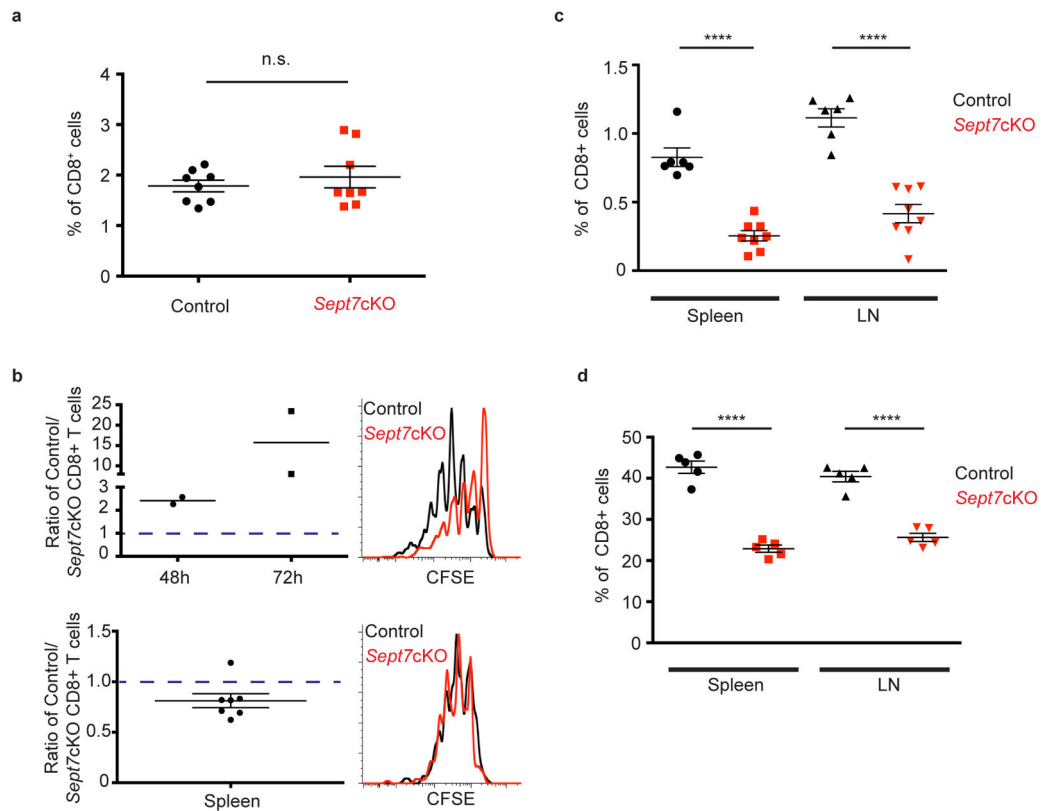


Figure 5. Septin deficiency differentiates APC- and cytokine-driven division *in vivo*

(a) Frequency of co-transferred control or *Sept7cKO* CD8⁺ OT-I T cells that expanded in draining inguinal lymph nodes of host mice that had been immunized subcutaneously with Dec205-OVA and anti-CD40 6d prior. (b) Naïve *Sept7cKO* and control CD8⁺ OT-I T cells were co-cultured with SL8-pulsed (100ng/ml) BMDCs *in vitro*, isolated 36h later, and either co-cultured *in vitro* with low-dose IL-2 (10U/ml) (top) or co-transferred to antigen-free host mice (bottom). Ratio of control to *Sept7cKO* live T cells 48h or 72h following *in vitro* culture, along with a representative CFSE dilution profile 48h after T cell isolation (top). Ratio of control to *Sept7cKO* T cells recovered from host mouse spleen 48h after co-transfer, as well as CFSE dilution of cells (bottom). *P value = 0.0351 with data analyzed with 1-sample *t*-test comparing distribution to theoretical mean of 1. (c) Frequency of CD45.2⁺ CD8⁺ OT-I T cells that expanded in the spleen and inguinal lymph nodes of CD45.1⁺ host mice following IL-2 complex delivery i.p. daily for 7 days. (d) Frequency of co-transferred *Sept7cKO* and control polyclonal CD8⁺ T cells in the spleen and skin-draining lymph nodes of sub-lethally irradiated mice. Each symbol represents an inguinal lymph node (left or right flank) from host mice (a), individual host mice (b–d), or an *in vitro* culture sample (b). Small horizontal lines demarcate the SEM. Data is representative of at least three independent experiments with n = 3–5 mice (a, d), or pooled from at least two (b; top) or three experiments with total n = 7 (b; bottom) or 8 mice (c). *P < 0.05, **P < 0.01, ***P < 0.001, ****P < 0.0001 with data analyzed with paired (a, d), or unpaired (c) *t*-test.

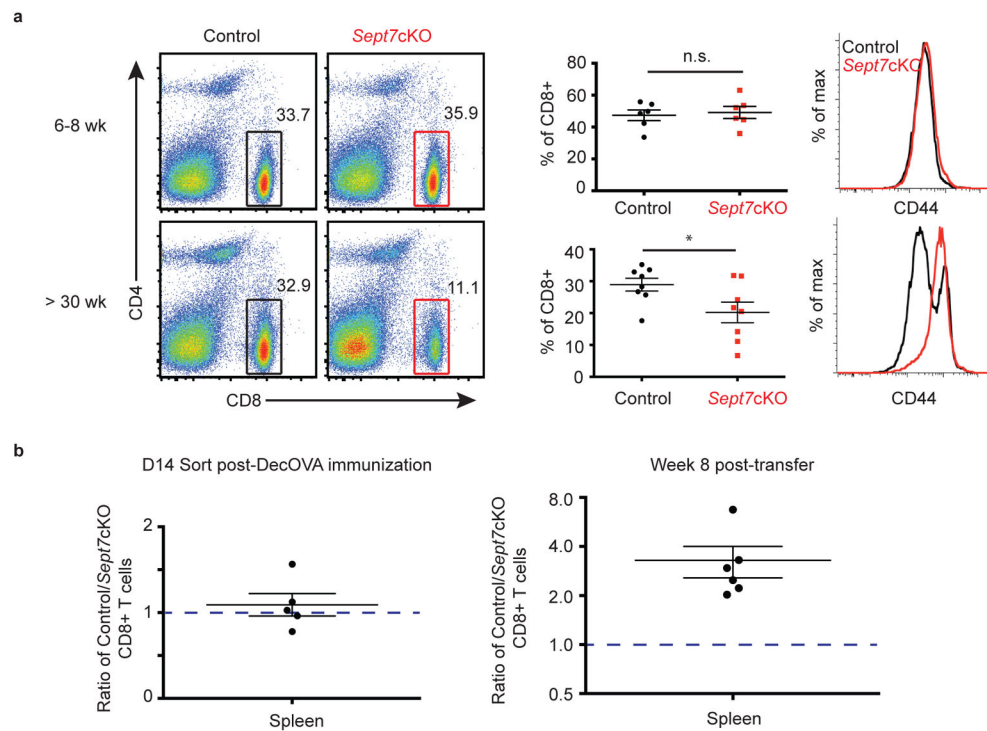


Figure 6. Septins are required for homeostatic maintenance of naïve and memory CD8⁺ T cells *in vivo*

(a) Frequency of CD8⁺ T cell population (**left**) and CD8⁺ T cell CD44 surface expression (**right**) in pooled lymph nodes of 6–8 week-old (**top**) or 6-month-old (**bottom**) OT-I mice. (b) *Sept7cKO* and control OT-I T cells were transferred to mice which were then immunized i.v. with DecOVA. OT-I T cells were sorted from immunized mouse spleen and lymph nodes 14d later, and co-transferred to antigen-free host mice. Ratio of control to *Sept7cKO* cells sorted from spleen 14d post-DecOVA immunization (**left**). Ratio of control to *Sept7cKO* T cells recovered from spleens of antigen-free host mice 8 weeks after transfer (**right**). Non-significant P value (> 0.05) (**left**) and *P value = 0.0243 (**right**) with data analyzed with 1-sample *t*-test comparing distribution to theoretical mean of 1 (**b**). Each symbol represents an individual mouse (**a, b; right**) or an independent experiment (**b; left**). Small horizontal lines denote the SEM. Data is pooled from at least four independent experiments with total n = 8 (**a**), 5 (**b; left**), or 6 (**b; right**). *P < 0.05 with data analyzed with unpaired *t*-test (**a**).